EPJ Web of Conferences **259**, 11009 (2022) https://doi.org/10.1051/epjconf/202225911009
SQM 2021

Hyperon Global Polarization in Nucleus-Nucleus Collisions at sub-10-GeV Beam Energy

Yu Guo[1,2], *Jinfeng* Liao[3,*], *Enke* Wang[1,2,**], *Hongxi* Xing[1,2,***], and *Hui* Zhang[1,2,****]

[1]Guangdong Provincial Key Laboratory of Nuclear Science, Institute of Quantum Matter, South China Normal University, Guangzhou 510006, China.
[2]Guangdong-Hong Kong Joint Laboratory of Quantum Matter, South China Normal University, Guangzhou 510006, China.
[3]Physics Department and Center for Exploration of Energy and Matter, Indiana University, 2401 N Milo B. Sampson Lane, Bloomington, IN 47408, USA.

Abstract. In this contribution, we report AMPT model study for the hyperon global polarization in the heavy ion collision, especially in the interesting $\hat{O}(1 \sim 10)$ GeV energy region. We find a non-monotonic trend, with the global polarization to first increase and then decrease when beam energy is lowered from 27 GeV down to 3 GeV, with a maximum polarization signal located around $\sqrt{s_{NN}} = 7.7$ GeV. In addition, local polarization patterns are also computed in the same energy regime.

1 Introduction

Where can one find the fastest spinning fluid in the world? This is a question of general interest. From a fluid dynamical point of view, the most vortical fluid droplet needs to be large enough to enable a hydrodynamic behavior while small enough to rotate fast without violating the speed of light constraint. In 2017, the STAR collaboration reported the measurement of hyperon global polarization in heavy ion collisions [1], suggesting the subatomic fireball fluid created in these collisions as the most vortical fluid with an average vorticity on the order of $10^{21\sim22}\mathrm{s}^{-1}$. This finding was further confirmed by subsequent detailed measurements in [2–5]. In particular, the measured global spin polarization of produced hadrons can be quantitatively related to the angular momentum of the colliding system [6–10], which turns into complex fluid vorticity structures.

One notable feature of the hyperon global polarization measurement results is a strongly increasing trend from high beam energy at $\sqrt{s_{NN}} = 200$ GeV to low beam energy at $\sqrt{s_{NN}} = 7.7$ GeV. It is tempting to ask whether such a trend would continue further into the $\hat{O}(1)$ GeV range and at which beam energy the truly most vortical fluid will be located. This beam energy region is interesting to explore also because it pertains to a likely shift from a partonic-dominant fluid to a hadronic-dominant fluid. The possible consequence of such change on the global polarization phenomenon is important to understand. In this contribution, we

*e-mail: liaoji@indiana.edu
**e-mail: wangek@scnu.edu.cn
***e-mail: hxing@m.scnu.edu.cn
****e-mail: mr.zhanghui@m.scnu.edu.cn

explore these questions by carrying out a systematic study on the beam energy dependence of hyperon global polarization phenomenon with a transport model calculation, especially in the most interesting region of $\hat{O}(1 \sim 10)$ GeV beam energy.

2 Formalism

We use the multi-phase transport (AMPT) model [18, 19] to compute the Λ hyperon spin polarization in this work. The AMPT model allows us to collect the parton space-time $x = (t, \vec{x})$ information and hadron kinematic freeze-out information from AMPT model, and calculate the vorticity by using the finite difference method after averaging a sufficient number of events. Finally we incorporate the spin polarization effect upon the hadron formation.

The rotational polarization effect on particle spin in a relativistic fluid can be determined from the thermal vorticity $\varpi_{\mu\nu}$, which is defined as [11]:

$$\varpi_{\mu\nu} = -\frac{1}{2}\left(\partial_\mu \beta_\nu - \partial_\nu \beta_\mu\right) \tag{1}$$

where $\beta_\mu = u_\mu/T$ with $T = 1/\beta$ the local temperature. A related quantity is the kinetic vorticity defined by $\Omega_{\mu\nu} = -\frac{1}{2}(\partial_\mu u_\nu - \partial_\nu u_\mu)$. Obviously $\varpi_{\mu\nu} = \beta\left\{\Omega_{\mu\nu} - \left[(\beta\partial_\mu T)u_\nu - (\beta\partial_\nu T)u_\mu\right]\right\}$. The thermal vorticity differs from the $\Omega_{\mu\nu}/T$ by terms containing gradients of temperature, $\sim (\beta\partial_\mu T) = [(\partial_\mu T)/T]$. We use the energy density ϵ to evaluate such terms via $(\partial_\mu T)/T = (\partial_\mu \epsilon)/(4\epsilon)$ [14–16]. The hyperon global polarization is then determined from the following ensemble-averaged spin 4-vector of the produced Λ from the local thermal vorticity at its formation point as [1, 11, 12, 15, 17]:

$$S^\mu = -\frac{1}{8m}\epsilon^{\mu\nu\rho\sigma} p_\nu \varpi_{\rho\sigma}, \tag{2}$$

where p^ν and m are the four-momentum and mass of the produced hyperon, respectively.

In the present work, we extend such transport model calculations to the regime of $\sqrt{s_{NN}} = (3 \sim 10)$ GeV and examining the trend of global polarization observables.

3 Results

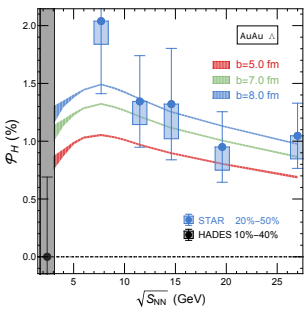

Figure 1. Λ global polarization signal as a function of collision beam energy with $|y_\Lambda| < 1.0$ and 0.4 GeV $< p_T <$ 3.0 GeV, for AuAu collisions at impact parameters $b = 5$ fm (red), 7 fm (green) and 8 fm (blue), with the bands representing statistical uncertainty from our simulation. Relevant measurements are also shown, with the STAR data from Ref.[1] and the HADES data from Ref. [20].

The key finding of this work is shown in Fig. 1, where the hyperon global polarization signal is computed as a function of collision beam energy, for AuAu collisions at three different impact parameters $b = 5$ fm (red), 7 fm (green) and 8 fm (blue). The plot includes

our calculations done for $\sqrt{s_{NN}} = 3, 4, 5, 6, 7.7, 9, 10, 11.5, 14.5, 19.6, 27$ GeV. This detailed and systematic scan in beam energy has allowed us to clearly identify a non-monotonic trend, with the global polarization to first increase and then decrease when beam energy is lowered from 27 GeV down to 3 GeV. The maximum polarization signal is found to locate around $\sqrt{s_{NN}} = 7.7$ GeV. The decrease toward 3 GeV is the combined effect of the decrease in both the vorticity itself and the average energy of produced hyperons at very low energy.

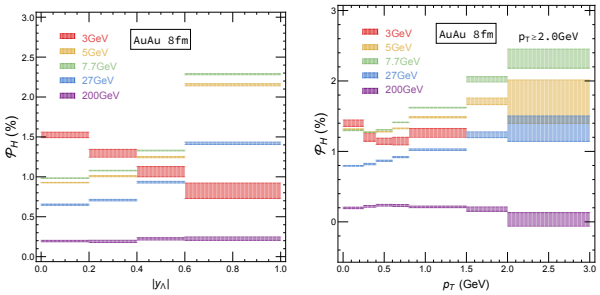

Figure 2. Λ global polarization signal for AuAu collisions at impact parameter $b = 8$ fm for a variety of collision beam energy from 200GeV down to 3GeV, with the bands representing statistical uncertainty from our simulation. Left: as a function of rapidity y; Right: as a function of transverse momentum p_T.

We've also computed the differential observables, with the dependence on rapidity and transverse momentum shown in the left and right panel of Fig. 2. A barely visible increase with rapidity at 200 GeV changes into a strong rising behavior at low energy down to 5 GeV, which then turns into a strong decrease with rapidity at 3 GeV. The dependence on the transverse momentum in the right panel of Fig. 2 also shows a similar pattern, in which the different beam energy dependence of vorticity and radial flow may play a role.

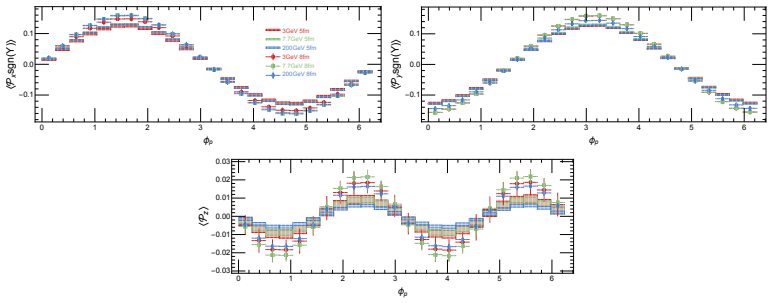

Figure 3. The dependence of hyperon local polarization components on the azimuthal angle ϕ_p for collisions with impact parameter $b = 5, 8$ fm and with beam energy $\sqrt{s_{NN}} = 3, 7.7, 200$ GeV, respectively. The bands (for $b = 5$fm) or error bars (for $b = 8$fm) represent statistical uncertainty from simulation.

In addition to global polarization, the local polarization patterns of produced hyperons provide another category of interesting observables [3, 21]. In Fig. 3, we show the dependence of all three components of the hyperon local polarization on the azimuthal angle ϕ_p with impact parameter $b = 5, 8$ fm, which are the first results of its kind for collision beam energies at 3 and 7.7 GeV. The results suggest that these azimuthal angular patterns are relatively insensitive to the collisional beam energy.

4 Summary and Discussion

In summary, we've performed a transport model (AMPT) study for the hyperon global polarization as well as local polarization patterns in the heavy ion collision. A systematic scan of the $\hat{O}(1 \sim 10)$ GeV energy region shows a non-monotonic trend with a maximum polarization signal located around $\sqrt{s_{NN}} = 7.7$ GeV. These results are of course model dependent. As the results were first reported, no experimental data between $3 \sim 7$ GeV were available yet. An agreement between this calculation and measurements could be an important confirmation of the fluid-vorticity-polarization scenario established at higher energy. On the other hand, if experimental data and the model results show discrepancy, it could be a very interesting indication of either a possible alternative mechanism of polarization generation or a possible shift of the dominant source hyperon production at those extremely low energies. In this sense, the hyperon polarization signal could offer valuable insights into such intriguing issues.

Acknowledgments

This work is supported in part by the Guangdong Major Project of Basic and Applied Basic Research (No. 2020B0301030008), by the National Natural Science Foundation of China under Grants No. 12022512, No. 12035007, No. 12047523, as well as by NSF Grant No. PHY-1913729 and the U.S. Department of Energy, Office of Science, Office of Nuclear Physics, within the framework of the Beam Energy Scan Theory (BEST) Topical Collaboration.

References

[1] STAR, L. Adamczyk *et al.*, Nature **548**, 62 (2017), arXiv:1701.06657.
[2] STAR, J. Adam *et al.*, Phys. Rev. C **98**, 014910 (2018), arXiv:1805.04400.
[3] STAR, J. Adam *et al.*, Phys. Rev. Lett. **123**, 132301 (2019), arXiv:1905.11917.
[4] STAR, J. Adam *et al.*, Phys. Rev. Lett. **126**, 162301 (2021), arXiv:2012.13601.
[5] ALICE, S. Acharya *et al.*, Phys. Rev. C **101**, 044611 (2020), arXiv:1909.01281.
[6] Z.-T. Liang and X.-N. Wang, Phys. Rev. Lett. **94**, 102301 (2005), arXiv:nucl-th/0410079, [Erratum: Phys.Rev.Lett. 96, 039901 (2006)].
[7] J.-H. Gao *et al.*, Phys. Rev. C **77**, 044902 (2008), arXiv:0710.2943.
[8] S. A. Voloshin, (2004), arXiv:nucl-th/0410089.
[9] B. Betz, M. Gyulassy, and G. Torrieri, Phys. Rev. C **76**, 044901 (2007), arXiv:0708.0035.
[10] F. Becattini, F. Piccinini, and J. Rizzo, Phys. Rev. C **77**, 024906 (2008).
[11] F. Becattini, L. Bucciantini, E. Grossi, and L. Tinti, Eur. Phys. J. C **75**, 191 (2015).
[12] F. Becattini, I. Karpenko, M. Lisa, I. Upsal, and S. Voloshin, Phys. Rev. C **95**, 054902 (2017).
[13] Y. Jiang, Z.-W. Lin, and J. Liao, Phys. Rev. C **94**, 044910 (2016), arXiv:1602.06580, [Erratum: Phys.Rev.C 95, 049904 (2017)].
[14] S. Shi, K. Li, and J. Liao, Phys. Lett. B **788**, 409 (2019), arXiv:1712.00878.
[15] H. Li, L.-G. Pang, Q. Wang, and X.-L. Xia, Phys. Rev. C **96**, 054908 (2017).
[16] X.-L. Xia, H. Li, Z.-B. Tang, and Q. Wang, Phys. Rev. C **98**, 024905 (2018).
[17] D.-X. Wei, W.-T. Deng, and X.-G. Huang, Phys. Rev. C **99**, 014905 (2019).
[18] Z.-W. Lin, C. M. Ko, B.-A. Li, B. Zhang, and S. Pal, Phys. Rev. C **72**, 064901 (2005), arXiv:nucl-th/0411110.
[19] Z.-W. Lin, Phys. Rev. C **90**, 014904 (2014), arXiv:1403.6321.
[20] HADES, F. J. Kornas, Springer Proc. Phys. **250**, 435 (2020).
[21] F. Becattini and I. Karpenko, Phys. Rev. Lett. **120**, 012302 (2018), arXiv:1707.07984.